Journal of Materials Science: Materials in Medicine (2019) 30:42
https://doi.org/10.1007/s10856-019-6245-7

BIOMATERIALS SYNTHESIS AND CHARACTERIZATION

Original Research

Impact of sterilization by electron beam, gamma radiation and X-rays on electrospun poly-(ε-caprolactone) fiber mats

Dominik de Cassan[1] · Anna Lena Hoheisel[2,3] · Birgit Glasmacher[2,3] · Henning Menzel[1]

Received: 9 January 2019 / Accepted: 13 March 2019 / Published online: 27 March 2019

Abstract

Biodegradable polymers such as polycaprolactone (PCL) are increasingly used for electrospinning substrates for tissue engineering. These materials offer great advantages such as biocompatibility and good mechanical properties. However, in order to be approved for human implantation they have to be sterilized. The impact of commonly used irradiation sterilization methods on electrospun PCL fiber mats was investigated systematically. Electron beam (β-irradiation), gamma and X-ray irradiation with two different doses (25 and 33 kGy) were investigated. To determine the impact on the fiber mats, mechanical, chemical, thermal properties and crystallinity were investigated. Irradiation resulted in a significant decrease in molecular weight. At the same time, crystallinity of fiber mats increased significantly. However, the mechanical properties did not change significantly upon irradiation, mostly likely because effects of a lower molecular weight were balanced with the higher degree of crystallinity. The irradiation effects were dose dependent, a higher irradiation dose led to stronger changes. Gamma irradiation seemed to be the least suited method, while electron beams (β irradiation) had a lower impact. Therefore, β irradiation is recommended as sterilization method for electrospun PCL fiber mats.

Graphical Abstract

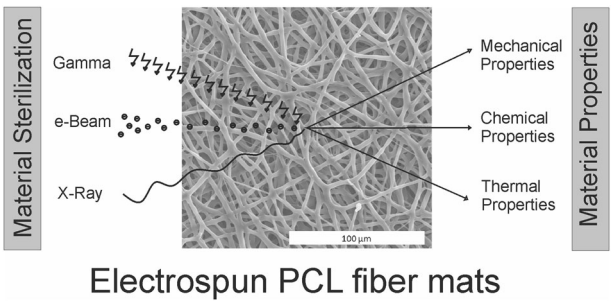

1 Introduction

Pathogens on the surface or within a biomedical device can cause severe infections and can even lead to an explantation surgery. Hence biomedical devices intended for human implantation require sterilization in order to fulfill regulatory issues. These regulatory aspects, based on established standards, are set by organizations such as the US Food and Drug Administration or the Medical Device Directive for manufacturers within the EU [1, 2].

Several sterilization methods have been established over past decades. These methods include steam processing/autoclaving [1], treatment with ethylene oxide [3], plasma sterilization [4], as well as irradiation with

Supplementary information The online version of this article (https://doi.org/10.1007/s10856-019-6245-7) contains supplementary material, which is available to authorised users.

✉ Henning Menzel
h.menzel@tu-bs.de

[1] Institute for Technical Chemistry, Braunschweig University of Technology, Braunschweig, Germany

[2] Institute for Multiphase Processes, Gottfried Wilhelm Leibniz Universität Hannover, Hannover, Germany

[3] Lower Saxony Centre for Biomedical Engineering, Implant Research and Development (NIFE), Hannover, Germany

electron beams (beta irradiation) [5], gamma-radiation [6] or X-rays [7]. The sterilization method has to be chosen according to materials used for implants, because sterilization itself can be inappropriate, ineffective or even destructive [8–11].

Electrospinning is a common technique for production of structured scaffolds (fiber mats), which are similar to extracellular matrix (ECM) (for tissue-engineering applications) [12–14]. These fiber mats are very versatile in application and for example used to produce wound dressings [15], nerve conduits [16], vascular grafts [17], drug delivery systems [18] and implants for tendon/ligament-to-bone interfaces [19]. In the laboratory, such electrospun scaffolds are typically sterilized using EtOH immersion or UV irradiation. However, for use as an implantable biomedical device, these sterilization methods are not approved by regulatory bodies [20, 21]. The use of electrospun scaffolds for biomedical devices is therefore not permissible using these simple sterilization strategies. On the other hand, it has been shown that gamma irradiation can cause significant damage to electrospun polymeric scaffolds. In general high energy radiation like gamma-rays can lead to polymer chain scission and, depending on the polymer, result in lower molecular weight or crosslinking [22, 23]. However, these effects do not necessarily lead to lower mechanical or biological performance. Bosworth et al. [14] and Augustine et al. [24] produced various PCL scaffolds by different electrospinning approaches and used gamma-radiation for sterilization. Bosworth et al. found in their studies that γ-irradiation lowers the molecular weight and ultimate tensile stress of PCL fiber mats depending on the irradiation dose used [14]. Augustine et al. found that a low irradiation dose first leads to improved mechanical properties but higher irradiation doses ultimately led to a decrease [24].

Due to relatively low melting temperature of PCL of 60 °C some sterilization methods could damage the material or implant structure. Hence steam processing and autoclaving techniques are not applicable for PCL. This study therefore focusses on comparing the impact of three established and approved low temperature sterilization techniques on electrospun PCL scaffolds: Electron beam (β), gamma radiation (γ) and X-rays. To investigate a possible dose dependent effect, two irradiation doses are used including the commonly used dose for medical devices sterilization of 25 kGy. While static tensile testing was carried out to determine changes regarding materials mechanical properties, size exclusion chromatography (SEC) was used to check for changes in molecular weight and differential scanning calorimetry (DSC) measurements to determine degree of crystallization and changes in thermal properties.

2 Materials and methods

Unless otherwise stated all chemicals used were purchased from Sigma-Aldrich. PCL ($M_n = 80{,}000$) was also purchased from Sigma-Aldrich (Darmstadt, Germany). 2,2,2-Trifluoroethanol (TFE) was purchased from ABCR (Karlsruhe, Germany).

2.1 Electrospinning of PCL

A 17% (w/v) PCL in 2,2,2-trifluoroethanol (TFE) solution was loaded into a syringe connected by polyvinylchloride (PVC) tubing to a spinneret. A rotating aluminum drum covered with polytetrafluoroethylene (PTFE) coated baking paper (ja!, REWE, Germany) was used as collector. Scaffolds were produced with a voltage of 20 kV at a circumferential speed of either 2 m/s for non-aligned but randomly oriented fibers (r) or 8 m/s for aligned fibers (a). Spinneret to collector distance was set to 20 cm and the solution flow rate to 3 ml/h. The electrospinning process ran for 2 h.

2.2 Sterilization

Prior to sterilization specimens were cut into uniform strips using a rotary cutter (Dahle, Germany). Specimens had a width of 10 mm and a free tensile test length of 40 mm in rotary direction. A set of unsterilized specimens served as control. Sterilization was carried out by Mediscan (Seibersdorf, Austria). Each of the three irradiation types (β, γ and X) was tested with two irradiation doses (25 and 33 kGy).

2.3 Scaffold morphologies

Scaffolds were imaged with SEM (Hitachi S-3400N, Tokyo, Japan) to investigate alignment of fibers within two sample types of non-aligned and aligned fiber mats. SEM images were analyzed with an image analysis software (AxioVision, Carl Zeiss, Jena, Germany).

2.4 Mechanical characterization

Static tensile testing was carried out using a universal testing machine (5655, Instron, Norwood, USA). Specimens were mounted to the universal testing machine with pneumatic grips and tested with a crosshead speed of 40 mm/min with a load cell of 500 N at 20 °C. Specimens were stretched until failure.

Thickness of specimens was determined by cutting samples with a cryotome and taking images with SEM (Hitachi S-3400N, Tokyo, Japan). Images were analyzed with image analysis software (AxioVision, Carl Zeiss, Jena,

Germany) and average thickness was calculated at about 246 ± 49 µm.

An algorithm was developed using Scilab software (Version 5.4.1, ESI Group, Rungis, France) to compute the data of the static testing and calculate ultimate tensile stress and elongation at break automatically [25].

2.5 Dynamic light scattering (DLS) and zeta-potential

Particle size was measured with a Zetasizer Nano ZS from Malvern Instruments (Malvern, UK). Size measurements were carried out in disposable sizing cuvettes (DTS0012) at 20 °C. For data analysis Malvern Zetasizer Software Version 7.03 was used.

2.6 Differential scanning calorimetry (DSC)

Differential scanning calorimetry (DSC) measurements were carried out on a Netzsch DSC204 Phoenix connected to Netzsch TASC 414/3A controller equipped with CC-200 cooling controller from Netzsch (Selb, Germany). PCL scaffolds were sealed in alumina pans with pierced lid and exposed to a double heating cycle: Samples were heated up from room temperature to 120 °C with a heating rate of 10 °C/min. Subsequently, samples were cooled down to −100 °C with a cooling rate of 10 °C/min and heated up again to 120 °C with a heating rate of 10 °C/min. Proteus thermal analysis software (Netzsch) was used to quantify melting temperature as peak temperature (T_m), enthalpy of fusion (H_F), glass transition temperature (T_g) and change in heat capacity at glass transition (Δc_p). Both heating cycles were evaluated. For quality control reasons, another set of thermograms was recorded on a TA Q2000 by TA instruments (New Castle, USA). Heating cycles and sample preparation are identical to the ones performed on Netzsch DSC. Universal Analysis software (TA Instruments) was used to quantify melting temperature (T_m), enthalpy of fusion (H_F), glass transition temperature (T_g) and change in heat capacity at glass transition (Δc_p). Data was merged by averaging for a comprehensive overall median value, since all measured sets were identical.

2.7 Size exclusion chromatography (SEC)

SEC measurements were carried out on a set of PSS GRAM columns (precolumn, 5 µm, 2 × 1000 Å, 5 µm) (Mainz, Germany) with THF as eluent at 40 °C with a flow rate of 1 mL/min. Injection volume was 100 µL with a sample concentration of 2 mg/mL. Chromatograms were recorded with a refractive index detector Agilent 1260 Infinity from Agilent (Santa Clara, USA) at 35 °C and a viscosity detector PSS DVD1260 from PSS (Mainz, Germany) at 30 °C which allowed using an universal calibration. WinGPC Unichrom software (PSS) was used to process the chromatograms.

3 Results

Electrospun PCL fiber mats were sterilized using electron beam (β), gamma radiation (γ) and X-rays (X-ray) at doses of 25 and 33 kGy each. It has been reported that γ-radiation damages PCL and changes both its mechanical and chemical properties [14, 24]. Since the methods used here, namely electron beam and X-rays sterilization differ in their photon energy [11, 26], they might have less impact on the material properties of electrospun PCL fiber mats. Changes regarding mechanical and thermal properties were monitored. Preliminary studies, even though not comprehensively performed, proved that sterilization itself did not negatively affect biocompatibility of the scaffolds as shown in literature [14].

3.1 Scaffold properties

Fiber mats were produced with different collector speeds, in order to control the alignment of the fibers. The mats were investigated regarding the fiber orientation by scanning electron microscopy (SEM) (see Fig. 1). Fiber mats produced with a higher collector speed showed alignment, while fiber mats produced with a low collector speed were

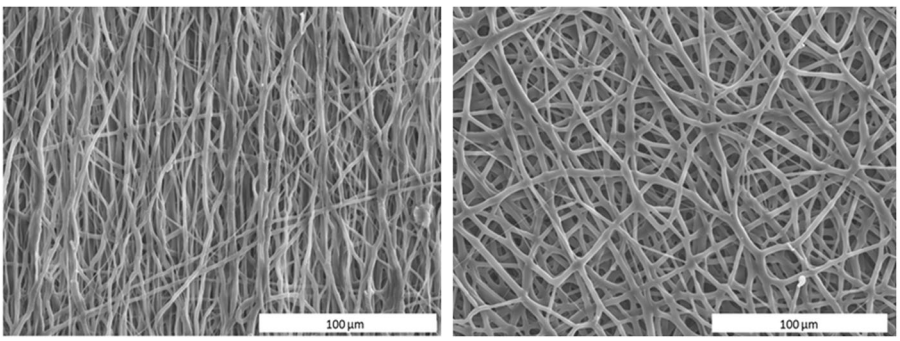

Figure 1 SEM micrographs of an aligned (left) and non-aligned (right) PCL fiber mat

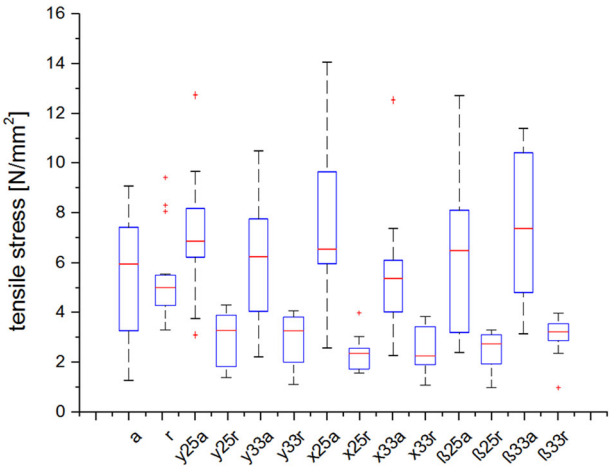

Figure 2 Tensile stress ($n \geq 10$) for electrospun PCL scaffolds. Shown are control samples for aligned (a) and non-aligned (r) fibers and sterilized samples. Use of gamma (γ), X-ray (x) and beta (ß) radiation at 25 and 33 kGy. Doted lines display the median values for control sets of aligned (red) and non-aligned (blue) samples

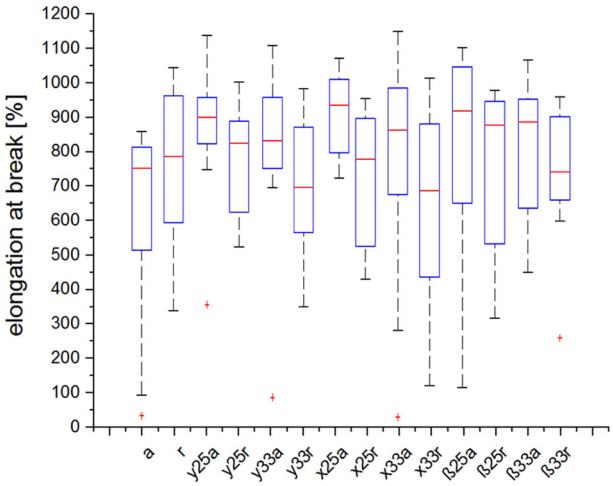

Figure 3 Elongation at break ($n \geq 10$) for electrospun PCL scaffolds. Shown are control samples for aligned (a) and non-aligned (r) fibers and sterilized samples. Use of gamma (γ), X-ray (x) and beta (ß) radiation at 25 and 33 kGy. Doted lines display the median values for control sets of aligned (red) and non-aligned (blue) samples

non-aligned (see Supplementary Information Figs 10 and 11). The fiber diameter of the aligned (*a*) PCL fiber mats was 2.1 ± 0.6 µm and for the non-aligned (random, *r*) 2.2 ± 0.5 µm. Furthermore, SEM images proved that fiber mats were of consistent quality and showed a homogenous fiber morphology distribution.

3.2 Mechanical properties

PCL scaffolds were tested to determine ultimate tensile strength and elongation at break. For the control set, each kind of irradiation, and both doses at least ten specimens were tested following the protocol developed by Zernetsch [27]. Data were computed with a self-developed SciLab algorithm and plotted as boxplots for non-aligned and aligned PCL scaffolds separately (see Fig. 2). The boxes for both types of untreated fiber mats showed a high width, which implied a great spread of the data. Median of ultimate tensile strength was 6 N/mm² and 5 N/mm² for the non-aligned and aligned scaffolds, respectively. After irradiation, the ultimate tensile strength of non-aligned PCL scaffolds decreased for all irradiation types and intensities compared to control group to about 2/3 of the control value. Such a decrease in the mechanical strength has been observed by Bosworth et al. as well [14]. The median values were in range of 2.4–3.3 N/mm². The effects seemed not to be dependent on dose or type of irradiation. For the aligned fiber mats, however, the median values for ultimate tensile strength varied between 5.5 and 7.5 N/mm² and therefore remained more or less unchanged after sterilization.

The elongation at break (see Fig. 3) was 775% for non-aligned and 750% for aligned PCL fiber mats before sterilization. For the non-aligned samples, no effect of the sterilization was observed. However, for aligned samples, a slight increase in elongation at break was measured after irradiation from 750% for control to ~900% for irradiated samples. Again, no significant effects of the dose or type of irradiation on the mechanical properties were observed.

3.3 Size exclusion chromatography (SEC)

PCL of sterilized fiber mats was checked for changes in molecular weight after sterilization. Chromatograms were recorded on a THF-SEC using refractive index and viscosity detector allowing for universal calibration. Each sample was tested at least three times ($n \geq 3$). Numerical average and standard deviation were calculated and two sample *t*-tests were performed to check for significant differences by using degrees of freedom and determining the corresponding *p*-values (* ≤ 5%, ** ≤ 1%, *** ≤ 0.1%, n.s. = not significant).

Figure 4 shows two exemplary SEC chromatograms and their refractive index detectors signals. In both cases, only one signal with a polydisperse molecular weight distribution was observed. According to manufacturer, the PCL used for the fiber mat production had a molecular weight of 80,000–120,000 g/mol. This was verified by our SEC measurements, which showed that unsterilized but processed PCL had an average molecular weight $\bar{M}_n$ of 95,000 g/mol. The PCL from fiber mats sterilized with gamma radiation at a dose of 33 kGy showed a significant higher retention time compared to PCL from a non-sterilized sample corresponding to lower a $\bar{M}_n$ of 67,500 g/mol.

Such a reduction in molecular weight was established for all PCL samples from sterilized fiber mats (see Fig. 5). The

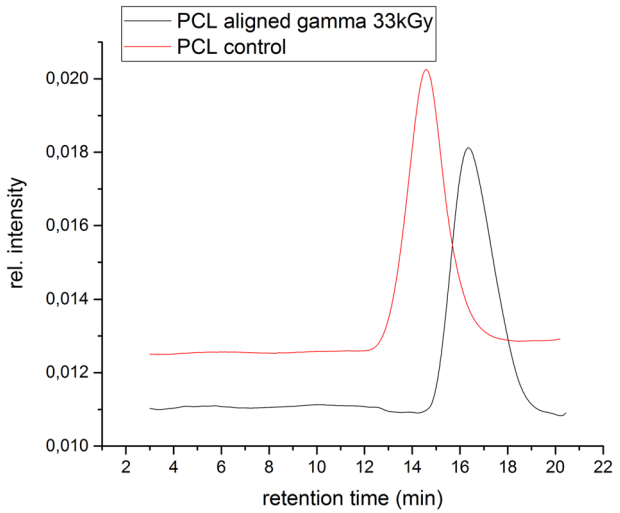

Figure 4 THF-SEC chromatogram for PCL (red) and PCL, sterilized with gamma irradiation at a dose of 33 kGy (black)

higher the irradiation dose the more chain cleavage took place and the lower the average molecular weight.

3.4 Thermal properties and crystallinity

Sterilized fiber mats were analyzed using differential scanning calorimetry (DSC) techniques on two different DSC setups with three identical runs each to verify the results. Exemplary thermograms are shown in Fig. 6. It can be seen that thermograms resulting from the 1st and 2nd heating cycle differed slightly, which was due to the different thermal history of the material. While the sample in the first heating cycle was material that crystallized in the electrospinning process by fast evaporation of a solvent, the sample in the second heating cycle crystallized during a controlled cooling process. Thus, only the first heating cycle allowed to draw conclusions about the actual crystallinity of fiber mats, while the second heating cycle probes the ability to crystallize. Furthermore, for the first heating cycle a fibrous material is used, which might have limited thermal contact with the aluminum pan and therefore can cause artefacts. Unless otherwise noticed, all data and conclusions in the following chapter are drawn from the 2nd DSC heating cycle and therefore depict the materials general capability to crystallize.

Figure 6 depicts the differences between 1st and 2nd heating cycle. In both cases, a clearly defined peak was visible. However, for the second heating cycle the melting started earlier and the melting peak was broader. Furthermore, the melting point measured as peak temperature was somewhat lower.

Comparing thermograms of a sterilized sample (µ-irradiation, 33 kGy) and non-irradiated but processed PCL as a control (see Fig. 7), differences in height of melting peak

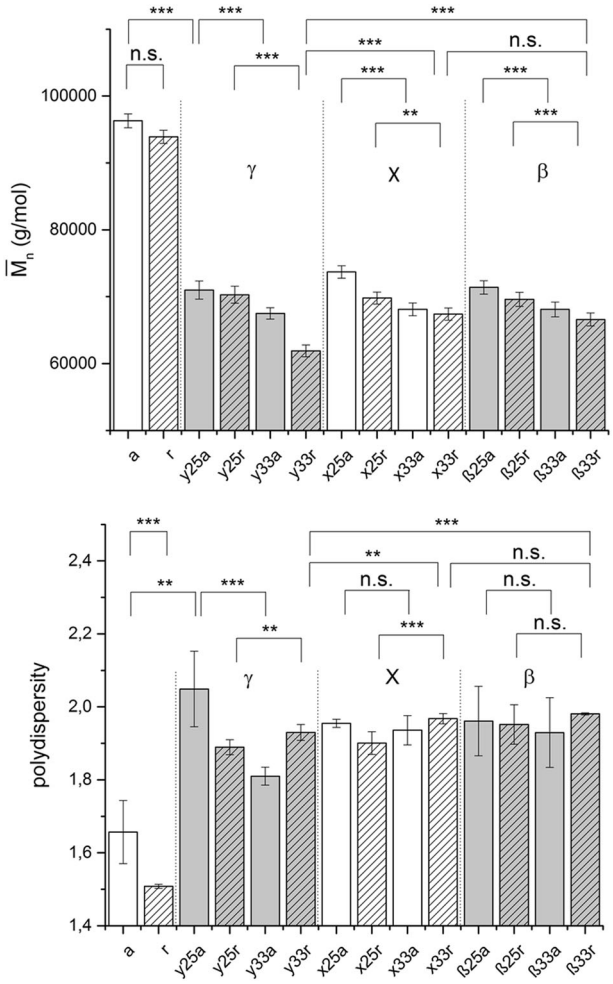

Figure 5 (top) molecular weights ($\overline{M}_n$) of sterilized scaffolds determined by THF-SEC for sterilized PCL fiber mats ($n \geq 3$, SD). (bottom) polydispersity of sterilized PCL scaffolds determined by THF-SEC ($n \geq 3$). Shown are control samples for aligned (a) and non-aligned (r) fibers and sterilized samples. Use of gamma (γ), X-ray (x) and beta (ß) radiation at 25 and 33 kGy. Statistics was performed using two sample *t*-test (* ≤ 5%, ** ≤ 1%, *** ≤ 0.1%, n.s. = not significant)

and, therefore, probably a difference in enthalpy of fusion was observed. Since all measurements looked similar and showed peaks in the same regions, data were processed with an automated procedure to compare them. Thermograms were evaluated regarding melting point T_m, enthalpy of fusion ΔH_F, glass transition temperature T_g and the change in heat capacity Δc_p. T-testing was performed to check for significance of changes against control group and between irradiation types and doses.

The aligned fibers had a higher melting temperature compared to randomly oriented fibers. Sterilization led to an increase in average melting temperature of about 1–2 °C at a dose of 33 kGy.

Besides melting temperature, also glass transition temperatures were evaluated. In some cases, a lower T_g was observed for PCL from sterilized samples (see Fig. 8

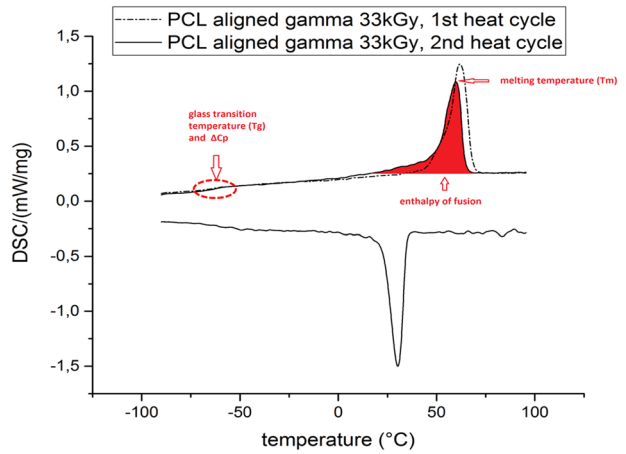

Figure 6 exemplary DSC thermogram of PCL sample sterilized with gamma irradiation at dose of 33 kGy. Shown are the 1st (dotted line), 2nd heating cycle (solid line) and relevant measurement points for sample evaluation

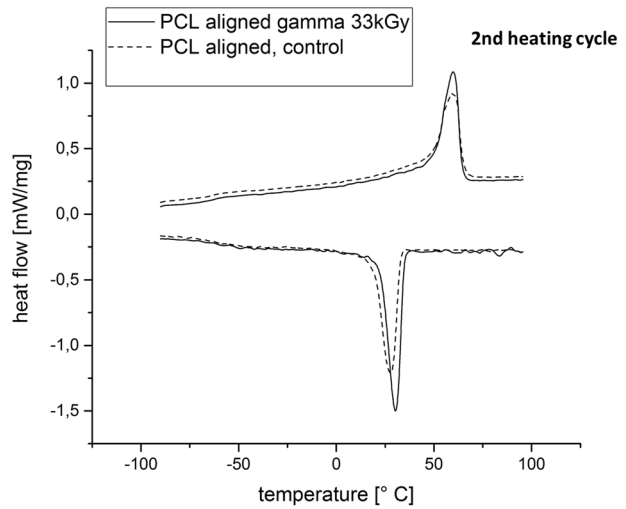

Figure 7 DSC thermogram showing differences between a sterilized (γ-radiation, 33 kGy) PCL sample (solid line) and an unsterilized PCL sample acting as control group (dotted line)

(bottom)). However, changes are small and in most cases statistically not significant. No clear trend was observed for samples irradiated with different doses. In addition, the type of radiation did not influence T_g in a consistent manner.

Change in heat capacity (Δc_p) was evaluated since it is indicating the fraction of amorphous material. It was observed that Δc_p was lowered significantly after irradiation treatment. This effect was dependent on dose and type of irradiation. Δc_p was lowered from 0.25 J/g*K for non-aligned unsterilized samples to a minimum of 0.17 J/g*K for X-radiation and a dose of 33 kGy.

Degree crystallization (X_c) can be estimated from the ratio of measured $\Delta H_F(T_m)$ (see Supplementary Information Fig. 14) and the enthalpy of fusion of a completely

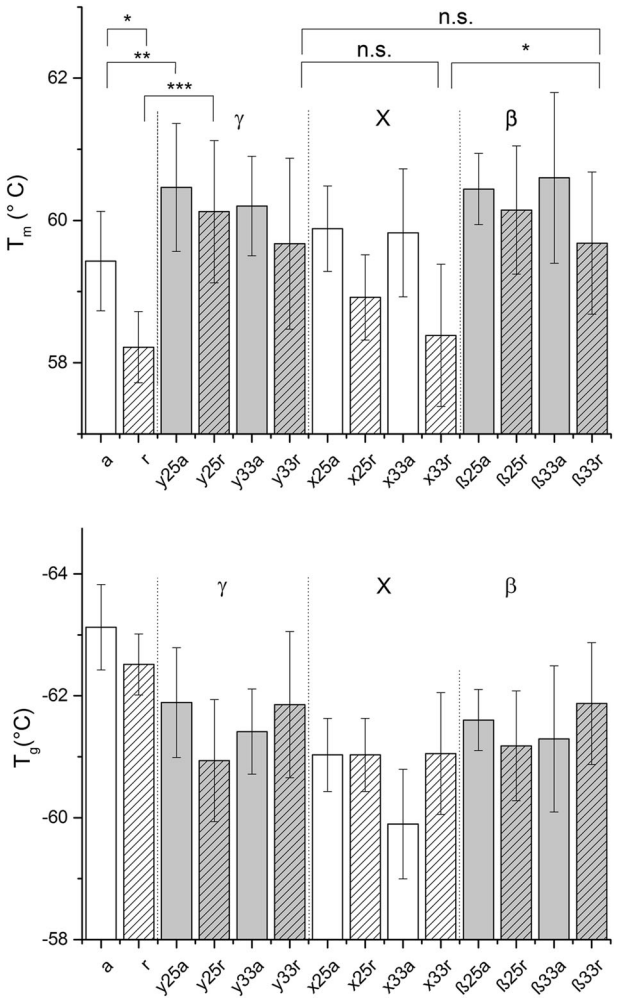

Figure 8 (top) T_m for sterilized PCL fiber mats. (bottom) T_g for sterilized PCL fiber mats ($n \geq 6$, SD). Shown are control samples for aligned (a), non-aligned (r) fibers and sterilized samples. Use of gamma (y), X-ray (x) and beta (ß) radiation at 25 and 33 kGy. Statistics ($n = 6$) was performed using two sample t-test (* ≤ 5%, ** ≤ 1%, *** ≤ 0.1%, n.s. = not significant)

crystalline material $\Delta H_F^0(T_m^0)$:

$$X_c = \frac{\Delta H_F(T_m)}{\Delta H_F^0(T_m^0)} \quad (1)$$

Enthalpy of fusion of completely crystalline PCL $\Delta H_F^0(T_m^0)$ has been reported as 139.3 J*g^{-1} [28]. With these data, the degree of crystallinity was calculated for all samples and depicted in Fig. 9. Again, it was observed that aligned fibers were more crystalline than randomly oriented fibers, although the second heating cycle was evaluated.

Furthermore, it was observed that all types and doses of irradiation used for sterilization led to a significant increase in crystallinity, as it was already expected after evaluation of Δc_p (see above). This effect was significantly stronger for irradiation with electrons and X-rays compared to

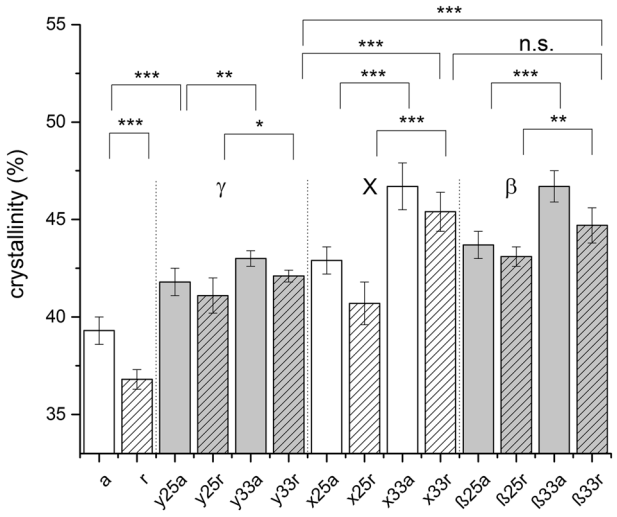

Figure 9 crystallinity of sterilized PCL samples ($n \geq 6$, SD). Shown are control samples for aligned (a) and non-aligned (r) fibers and sterilized samples. Use of gamma (γ), X-ray (x) and beta (ß) radiation at 25 and 33 kGy. Statistics ($n = 6$) was performed using two sample *t*-test (* ≤ 5%, ** ≤ 1%, *** ≤ 0.1%, n.s. = not significant)

γ-irradiation. The increase in crystallinity amounted to up to 9.9% for X-ray- and β-irradiation at 33 kGy.

4 Discussion

Aligned and non-aligned PCL scaffolds were produced and evaluated. Fiber alignment was evaluated by SEM imaging, as shown in Fig. 1. It was shown that homogenous fibers of aligned and non-aligned nature (see Supplementary Information Figs 11 and 12) were produced. It is known that this orientation of fibers comes along with various changes in the material properties such as mechanical properties, fiber diameter and crystallinity [29]. Furthermore fiber diameter was analyzed and showed slightly thinner fibers for aligned samples. This slight difference in fiber diameter might also influence the thermal properties and crystallinity after sterilization, however, the main influence of the fiber orientation is on mechanical properties.

PCL scaffolds were tested to determine ultimate tensile strength and elongation at break. ISO 13934 is a commonly used standard to determine tensile properties of fabrics, however for electrospun fiber structures a reliable standard for mechanical characterization does not exist [30]. Inconsistent testing of electrospun structures throughout the available literature creates obstacles for the comparison with results from other research groups and highlights the necessity for a uniform testing method. Therefore, Zernetsch developed a protocol for testing electrospun fiber mats and analyzing data, based on the norm ISO 527 for mechanical testing of plastics [27].

Augustine et al. [24] and Bosworth et al. [14] tested the influence of γ-sterilization on electrospun PCL scaffolds. Both groups worked with a replicate of 5 specimens. Using a static setup, Augustine et al. [24] produced highly disordered fiber mats, while Bosworth et al. [14] used a rotating drum with a circumferential speed of 3.77 m/s, which is significantly lower than the speed used here (8 m/s). In addition, electrospinning solutions and other process parameters were significantly different, as well as testing parameters.

Both groups found no significant difference of elongation at break before and after γ-irradiation treatment nor an influence of irradiation dose on the same. However, Augustine et al. [24] found that ultimate tensile stress of aligned scaffolds first increased with irradiation treatment compared to a non-sterilized control while decreasing at higher irradiation doses. Bosworth et al. [14] on the other hand showed that ultimate tensile stress decreased when non-aligned scaffolds were exposed to irradiation while the dose showed no significant effect on ultimate tensile stress.

We observed that for non-aligned scaffolds upon sterilization the ultimate tensile strength decreased slightly (see Fig. 2), while elongation at break remained unchanged (see Fig. 3). On the other hand, for aligned scaffolds the ultimate tensile strength did not change significantly, while the elongation at break showed a trend for slightly higher median values, but with a large spreading of the data. Thus, in particular for the aligned fiber mats the results obtained were not completely in line with the findings of Augustine et al. and Bosworth et al. However, this was probably due to inconsistent electrospinning and tensile testing protocols.

High energy radiation does not only sterilize a medical device made from polymers, however, it can also result in a scission of the polymer chains [14]. Formation of radicals in the polymer matrix, due to chain scission, might also result in crosslinking or branching of polymer chains. Thus, SEC measurements were performed. These indicated a lower molecular weight ($\bar{M}_n$) after sterilization due to irradiation induced chain scission, as shown in Fig. 5. This was further substantiated by a change in polydispersity of the PCL from irradiated samples. We used *t*-testing to check for differences between aligned and non-aligned samples resulting from fiber diameter and alignment. In addition, irradiation types and different irradiation doses were tested for significant differences against each other and against non-sterilized control. As depicted in Fig. 5, polydispersity increased significantly after sterilization by high-energy irradiation, which was another indication for polymer chain scission [31, 32]. The loss in molecular weight is in line with the observations of Bosworth et al. [14]. Furthermore, an influence of the type of sterilization was observed. Once more, the different irradiation doses and types were tested against each other and against a non-sterilized control to

check for significant differences. γ-Irradiation with 33 kGy had the strongest impact and led to a significant molecular weight reduction ($\bar{M}_n$) of 30 ± 1%. The $\bar{M}_w$ (see Supplementary Information Fig. 13) decreased slightly as well. In general, γ-irradiation should have the highest capability to cleave the polymer chains because of its higher photon energy compared to β- and X-ray irradiation [11, 26]. However, also β- and X-ray irradiation resulted in chain scission and a reduction of $\bar{M}_n$ to 69,100 g/mol for β-radiation and 68,400 g/mol for X-ray for 33 kGy irradiation dose and aligned fiber mats, indicating that also here photon energy is high enough for some chain scission. However, the reduction in $\bar{M}_n$ is statistically significant less pronounced for β- and X-ray irradiation compared to the γ-irradiation. Therefore, these methods appeared more suitable for sterilization of medical products produced from PCL.

Irradiation and chain scission as primary reaction creates radicals, which in a secondary reaction can lead to crosslinking. However, SEC chromatograms showed no indication for crosslinking products, like a high molecular weight shoulder in the distribution. This could be because the solutions were filtered before SEC-analysis, which should remove any microgel particles. Therefore, DLS measurements were performed with non-filtered polymer solutions. This technique should be able to detect such microgels easily. However, no such particles were found, which concluded the presumption that no crosslinking occurred.

The significant reductions in average molecular weight were expected to result in a decrease in mechanical properties, which was not observed (see above). However, the reduced polymer chain length was presumed to be compensated in particular in the aligned fiber mats. The strength of a material strongly depends on the degree of crystallinity; therefore, thermal properties and crystallinity of the samples were investigated.

Thermal properties and crystallinity of materials fabricated for medical applications can be critical for their performance [2], especially due to relatively low melting point of PCL of 60 °C [33]. Considerable lowering of this melting point could lead to failure of the implant since human body temperature can reach up to 42 °C [34]. Hence sterilization method and dose should be chosen according to the lowest impact on the original material properties. As shown in Fig. 6, differences between 1st and 2nd heat cycle can be measured. These differences were attributed to a different size distribution of crystalline regions caused by different thermal history of the samples. Thermograms were evaluated regarding melting point T_m, enthalpy of fusion ΔH_F, glass transition temperature T_g and the change in heat capacity Δc_p. T-testing was performed to check for significance of changes against control group and between irradiation types and doses.

Aligned fibers showed a higher T_m compared to non-aligned ones, which might be due to increased crystallinity resulting from stretching of fibers in electrospinning process and associated improved orientation of polymer chains [29]. However, taking into account the changes were only significant for a few comparisons it can be concluded that all sterilization doses and techniques had no big impact on melting peak temperature of the materials (see Fig. 8 (top)). T_g was also not affected in a statistically significant and consistent manner (see Fig. 8 (bottom)).

Change in heat capacity (Δc_p) at glass transition is a measure for fraction of amorphous material in the sample. A small change in Δc_p indicates a low amorphous and therefore a high crystalline portion. Δc_p was lower for PCL from aligned fiber mats, indicating a smaller portion of amorphous material (see Fig. 10). This behavior was unexpected for PCL-samples, which have been processed in the same way except for some stretching of the fibers. In the second heating cycle thermal or mechanical history of the sample should have been eradicated. However, it has been shown that a memory effect regarding crystallinity, mainly due to remaining small crystallites, can be observed for polymers even after melting [35–37]. Therefore, even after melting the polymer once, a lower Δc_p for aligned samples as consequence of the stretching during electrospinning can be observed (see Fig. 5, top). Upon sterilization, Δc_p was reduced significantly, thus the fraction of amorphous material is reduced by the sterilizations methods used here. While type of irradiation used did not make very much of a difference, used dose had a strong influence. The higher the dose the lower Δc_p. T-testing showed that decrease in Δc_p is significant after sterilization for all tested irradiation types

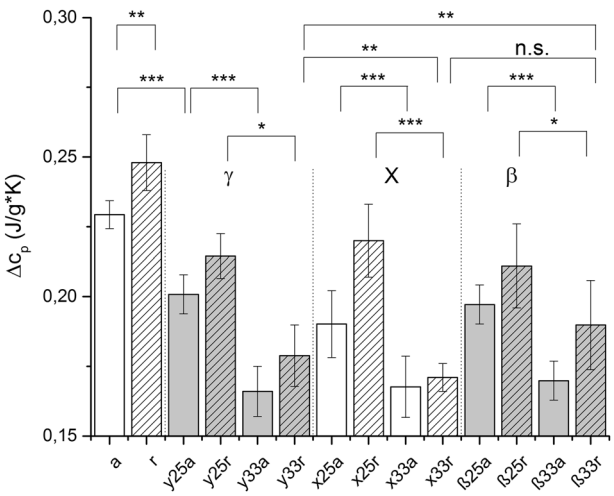

Figure 10 Change in heat capacity (Δc_p) for sterilized PCL fiber mats ($n \geq 6$, SD). Shown are control samples for aligned (a) and non-aligned (r) fibers and sterilized samples. Use of gamma (γ), X-ray (x) and beta (ß) radiation at 25 and 33 kGy. Statistics ($n = 6$) was performed using two sample *t*-test (* ≤ 5%, ** ≤ 1%, *** ≤ 0.1%, n.s. = not significant)

and doses. In conclusion, the evaluation of change in heat capacity at the glass transition indicated that used sterilization methods increased the degree of crystallinity. However, Δc_p is an indirect measure for degree of crystallinity and, therefore, heat of fusion ΔH_F (see Supplementary Information Fig. 14), the area of the melting peak, was evaluated as well.

ΔH_F is, beside X-ray investigations, probably the most direct access to degree of crystallinity. Samples with a high degree of crystallinity show a high ΔH_F, since crystalline regions need energy to break up their order and related intermolecular interactions. It was observed that melting of the polymers for a relatively short time did not eradicate ordering of the polymer chains completely. Although the polymer chains became mobile, the viscosity of melt was still very high and restructuring of the polymer chain conformation would have required a long time. The polymer however was cooled down before chain ordering due to the electrospinning process was completely eradicated (memory effect) [35–37]. A significant increase in crystallinity was observed after irradiation. This effect was once more dependent on dose or type of irradiation used (see Fig. 9). Irradiation seemed to affect and cleave the polymer chains, which should subsequently rearrange resulting in regions of higher crystallinity and therefore an overall smaller amorphous fraction. Since these effects were stronger at higher irradiation doses, a low dose should be chosen for medical devices sterilization.

Taken together, it can be clearly observed that sterilization by gamma (γ), X-ray (x) and beta (ß) radiation at 25 and 33 kGy led to changes regarding PCL's thermal properties and crystallinity. There was a significant influence of irradiation type used for sterilization on change in heat capacity (Δc_p) as well as on enthalpy of fusion (ΔH_F). The decrease in Δc_p and simultaneous increase in ΔH_F with irradiation, which are both statistically significant, indicated increasing crystallinity after sterilization. This was explained to be a consequence of chain scission and therefore reduced average molecular weight, which was established by SEC measurements. The shorter polymer chains can crystallize more easily resulting in higher degree of crystallinity. While on the one hand decreased molecular weight should also result in reduced mechanical strength, on the other hand a higher crystallinity should improve mechanical strength. Hence, maintained mechanical properties were a consequence of higher crystallinity compensating effects from polymer chain scission. Changes in T_m and T_g upon sterilization were minor and not consistently significant. It was observed that a higher irradiation dose during the sterilization process went along with a higher impact on the PCL scaffolds. Therefore, a low irradiation dose should be favorable to minimize changes in thermal properties and crystallinity of PCL.

It was shown that all three sterilization techniques had an impact on electrospun PCL scaffolds. Since none of the sterilization methods led to a failure of the fiber mats, all of them were proven to be generally applicable for sterilization of PCL fiber mats. However, use of β-irradiation seems preferable since it has less effect on the scaffolds compared to γ-irradiation. Furthermore medical device sterilization by β-radiation is easily accessible, cheap and more data are available for the method compared to sterilization by X-rays.

4.1 Conclusion and outlook

Sterilization of medical devices is inevitable to avoid post operation infections. However, sterilization methods have to be reliable and chosen according to the used materials properties. The impact of three different sterilization techniques (β, γ and X-ray) on electrospun PCL scaffolds was evaluated. It was shown that material properties of PCL in electrospun fiber mats were affected by all three sterilization techniques.

The irradiation led to a polymer chain scission and a decreased average molecular weight $\bar{M}_n$. The effect was more pronounced for higher irradiation doses. γ-irradiation with dose 33 kGy led to a decrease in $\bar{M}_n$ of around 30%. Polymer crosslinking as consequence of irradiation induced chain scission was ruled out since no indications for microgel particles were found in SEC and DLS measurements. Thermal properties and crystallinity of PCL were affected as well. While melting temperature and glass transition temperature were almost unchanged, change in heat capacity (Δc_p) and enthalpy of fusion (ΔH_F) were effected significantly. The changes indicated an improved crystallization process for sterilized samples. For mats with aligned fibers, ultimate tensile strength and elongation at break were even slightly increased while they remained unchanged for mats with non-aligned fibers. This slight improvement in mechanical properties of aligned scaffolds despite decreased polymer chain length was ascribed to the increase in crystallinity. The scission of long polymer chains into smaller ones led to an increased ability to form regions with a higher crystallinity and therefore higher mechanical strength, which overcomes negative effects of polymer chain scission. Electron beam had less effect on PCL than y-irradiation. Furthermore, it has been established already as a sterilization method. Therefore, electron beam sterilization is recommended for PCL fiber mats.

Acknowledgements This research project has been supported by the DFG FOR 2180 "Gradierte Implantate für Sehnen-Knochen-Verbindungen". Furthermore the authors would like to thank "Thünen-Institut für Agrartechnologie" for assistance in performing DSC measurements. The authors would like to thank Michael Bode and Alexander Becker (Institute for Multiphase Processes, Gottfried Wilhelm Leibniz Universität Hannover, Hannover, Germany) for discussions.

Compliance with ethical standards

Conflict of interest The authors declare that they have no conflict of interest.

Publisher's note: Springer Nature remains neutral with regard to jurisdictional claims in published maps and institutional affiliations.

References

1. Lerouge S, Simmons A. Sterilisation of biomaterials and medical devices. Woodhead Publishing series in biomaterials, no. 46. Philadelphia, PA: Woodhead Pub; 2012.
2. dos Santos V, Brandalise RN, Savaris M. Engineering of biomaterials. Cham: SpringerLink: Bücher. Springer; 2017.
3. Mendes GCC, Brandão TRS, Silva CLM. Ethylene oxide sterilization of medical devices: a review. Am J Infect Control. 2007;35:574–81. https://doi.org/10.1016/j.ajic.2006.10.014.
4. Hee Lee M, Joo Park B, Chang Jin S, Kim D, Han I, Park J-C. et al. Removal and sterilization of biofilms and planktonic bacteria by microwave-induced argon plasma at atmospheric pressure. New J Phys. 2009;11:115022. https://doi.org/10.1088/1367-2630/11/11/115022..
5. Benson RS. Use of radiation in biomaterials science. Nucl Instrum Methods Phys Res Sect B: Beam Interact Mater At. 2002;191:752–7. https://doi.org/10.1016/S0168-583X(02)00647-X.
6. Noah EM, Chen J, Jiao X, Heschel I, Pallua N. Impact of sterilization on the porous design and cell behavior in collagen sponges prepared for tissue engineering. Biomaterials. 2002;23:2855–61. https://doi.org/10.1016/S0142-9612(01)00412-4.
7. Govindaraj S. Systematic Review on Sterilization Methods of Implants and Medical Devices. Implants and Medical Devices. Int J ChemTech Res. 2015;8:897–911.
8. Hutmacher D, Hürzeler MB, Schliephake H. A review of material properties of biodegradable and bioresorbable polymers and devices for GTR and GBR applications. Int J Oral Maxillofac Implants. 1996;11:667–78.
9. Collier JP, Sperling DK, Currier JH, Sutula LC, Mayor MB. Impact of gamma sterilization on clinical performance of polyethylene in the knee. J Arthroplast. 1996;11:377–89. https://doi.org/10.1016/S0883-5403(96)80026-X.
10. Athanasiou K. Sterilization, toxicity, biocompatibility and clinical applications of polylactic acid/ polyglycolic acid copolymers. Biomaterials. 1996;17:93–102. https://doi.org/10.1016/0142-9612(96)85754-1.
11. Dai Z, Ronholm J, Tian Y, Sethi B, Cao X. Sterilization techniques for biodegradable scaffolds in tissue engineering applications. J Tissue Eng. 2016;7:2041731416648810. https://doi.org/10.1177/2041731416648810.
12. Hutmacher DW. Scaffolds in tissue engineering bone and cartilage. Biomaterials. 2000;21:2529–43.
13. Woodruff MA, Hutmacher DW. The return of a forgotten polymer—Polycaprolactone in the 21st century. Prog Polym Sci. 2010;35:1217–56. https://doi.org/10.1016/j.progpolymsci.2010.04.002.
14. Bosworth LA, Gibb A, Downes S. Gamma irradiation of electrospun poly(ε-caprolactone) fibers affects material properties but not cell response. J Polym Sci B Polym Phys. 2012;50:870–6. https://doi.org/10.1002/polb.23072.
15. Zahedi P, Rezaeian I, Ranaei-Siadat S-O, Jafari S-H, Supaphol P. A review on wound dressings with an emphasis on electrospun nanofibrous polymeric bandages. Polym. Adv. Technol. 2009;35. https://doi.org/10.1002/pat.1625
16. Lee B-K, Ju YM, Cho J-G, Jackson JD, Lee SJ, Yoo JJ. et al. End-to-side neurorrhaphy using an electrospun PCL/collagen nerve conduit for complex peripheral motor nerve regeneration. Biomaterials. 2012;33:9027–36. https://doi.org/10.1016/j.biomaterials.2012.09.008.
17. Hasan A, Memic A, Annabi N, Hossain M, Paul A, Khademhosseini A. et al. Electrospun scaffolds for tissue engineering of vascular grafts. Acta Biomater. 2014;10:11–25. https://doi.org/10.1016/j.actbio.2013.08.022.
18. Xue J, He M, Liu H, Niu Y, Crawford A, Zhang L. et al. Drug loaded homogeneous electrospun PCL/gelatin hybrid nanofiber structures for anti-infective tissue regeneration membranes. Biomaterials. 2014;35:9395–405. https://doi.org/10.1016/j.biomaterials.2014.07.060.
19. Font Tellado S, Balmayor ER, van Griensven M. Strategies to engineer tendon/ligament-to-bone interface: Biomaterials, cells and growth factors. Adv Drug Deliv Rev. 2015;94:126–40. https://doi.org/10.1016/j.addr.2015.03.004.
20. Rainer A, Centola M, Spadaccio C, Gherardi G, Genovese JA, Trombetta M. et al. Comparative study of different techniques for the sterilization of poly-L-lactide electrospun microfibers: effectiveness vs. material degradation. Int J Artif Organs. 2010;33:76–85.
21. Bhaskar P, Bosworth LA, Wong R, O'brien MA, Kriel H, Cartmell SH. et al. Cell response to sterilized electrospun poly(ε-caprolactone) scaffolds to aid tendon regeneration in vivo. J Biomed Mater Res A. 2017;105:389–97. https://doi.org/10.1002/jbm.a.35911.
22. Kudoh H, Sasuga T, Seguchi T. High-energy ion irradiation effects on polymer materials. In: Clough RL, Shalaby SW, (eds.). Irradiation of Polymers. Vol. 620. Washington, DC: American Chemical Society; 1996. p. 2–10.
23. Otaguro H, de Lima L, Parra DF, Lugao A. High-energy radiation forming chain scission and branching in polypropylene. Radiat Phys Chem. 2010;79:318–24. https://doi.org/10.1016/j.radphyschem.2009.11.003.
24. Augustine R, Saha A, Jayachandran VP, Thomas S, Kalarikkal N. Dose-dependent effects of gamma irradiation on the materials properties and cell proliferation of electrospun polycaprolactone tissue engineering scaffolds. international. J Polym Mater Polym Biomater. 2015;64:526–33. https://doi.org/10.1080/00914037.2014.977900.
25. Zernetsch H, Repanas A, Rittinghaus T, Mueller M, Alfred I, Glasmacher B. Electrospinning and mechanical properties of polymeric fibers using a novel gap-spinning collector. Fibers Polym. 2016;17:1025–32. https://doi.org/10.1007/s12221-016-6256-7.
26. Cottam E, Hukins DWL, Lee K. et al. Effect of sterilisation by gamma irradiation on the ability of polycaprolactone (PCL) to act as a scaffold material. Med Eng Phys. 2009;31:221–6. https://doi.org/10.1016/j.medengphy.2008.07.005.
27. Zernetsch H. Gezielte Beeinflussung der Mikro- und Makrostruktur polymerer Trägerstrukturen beim Elektrospinnen. Berichte aus dem IMP, Band 1. Garbsen: PZH Verlag; 2016.
28. Tiwari A, Raj B. Reactions and mechanisms in thermal analysis of advanced materials. Hoboken, New Jersey, Salem, Massachusetts: John Wiley & Sons; Scrivener Publishing; 2015.
29. Cipitria A, Skelton A, Dargaville TR. et al. Design, fabrication and characterization of PCL electrospun scaffolds—a review. J Mater Chem. 2011;21:9419. https://doi.org/10.1039/c0jm04502k.
30. Kancheva M, Toncheva A, Manolova N. et al. Enhancing the mechanical properties of electrospun polyester mats by heat treatment. Express Polym Lett. 2015;9:49–65. https://doi.org/10.3144/expresspolymlett.2015.6.

31. Luo Y, Li P, Jiang B. The estimation of the polydispersity index of molecular weight distribution with a radiation crosslinking technique: I. The effect of molecular weight distribution on the radiation crosslinking of polyethylene. Int J Radiat Appl Instrum C Radiat Phys Chem. 1987;29:415–8. https://doi.org/10.1016/1359-0197(87)90016-6.
32. O'Donnell JH, Rahman NP, Smith CA. et al. Chain scission and cross-linking in the radiation degradation of polymers: limitations on the utilization of theoretical expressions and experimental results in the pregel region. Macromolecules. 1979;12:113–9. https://doi.org/10.1021/ma60067a024.
33. Speranza V, Sorrentino A, de Santis F. et al. Characterization of the polycaprolactone melt crystallization: Complementary optical microscopy, DSC, and AFM studies. TheScientificWorldJournal. 2014;2014:720157. https://doi.org/10.1155/2014/720157.
34. Harrison TR, Longo DL, Kasper DL. et al. Harrison's principles of internal medicine. In: Dan L. Longo et al. Editors, 18th edn. New York: McGraw-Hill; 2012.
35. Martins JA, Zhang W, Brito AM. Origin of the melt memory effect in polymer crystallization. Polymer. 2010;51:4185–94. https://doi.org/10.1016/j.polymer.2010.07.010.
36. Chen X, Mamun A, Alamo RG. Effect of level of crystallinity on melt memory above the equilibrium melting temperature in a random ethylene 1-butene copolymer. Macromol Chem Phys. 2015;216:1220–6. https://doi.org/10.1002/macp.201500068.
37. Muthukumar M. Communication: Theory of melt-memory in polymer crystallization. J Chem Phys. 2016;145:31105. https://doi.org/10.1063/1.4959583.